1680 *Chem. Mater.* **2010,** *22,* 1680–1685
DOI:10.1021/cm9031607

CHEMISTRY OF MATERIALS
Article

Melting Characteristics of Superlattices of Alkanethiol-Capped Gold Nanoparticles: The "Excluded" Story of Excess Thiol

Deepti S. Sidhaye and B. L. V. Prasad*

Materials Chemistry Division, National Chemical Laboratory, Pune 411 008, India

Received October 14, 2009. Revised Manuscript Received January 13, 2010

Melting characteristics of gold nanoparticle superlattices obtained from nanoparticles capped by alkanethiols of different chain lengths (octane, dodecane and hexadecane) have been investigated. The alkanethiol capped nanoparticles were synthesized by the well-established digestive ripening method. It is observed that as the chain length of the thiol increases, the propensity to form superlattices decreases and the melting of the superlattice is observed at lower temperature. However, the formation of the 3D superlattice is critically dependent on the presence of "excess" thiol as determined from thermogravimetric and transmission electron microscope analysis. In the absence of "excess" thiol, only 2D hexagonally close-packed arrangements were seen.

Introduction

Gold nanoparticles have always been in the spotlight of research due to the bountiful applications they offer.[1] Functionalization of the particle surface is a prerequisite for many of the applications where the nature of the capping ligand plays a very important role. Many researchers have been synthesizing ligand protected gold nanoparticles. After the pioneering work of Mulvaney et al.[2] and Brust et al.,[3] the synthesis and characterization of alkanethiol protected gold nanoparticles has been a major area of research.[4,5] Here, in many instances, if the size distribution of the synthesized particles is sufficiently narrow, a self-assembly of the particles leading to the formation of ordered 2D or 3D superlattices occurs.[6] In the recent past, the formation of such superlattices have engrossed the attention of many research groups.[7] Nanoparticle superlattices can be composed of a single[8] or two different materials, e.g., binary superlattices.[9] Such assemblies are analogous to their atomic and molecular crystal cousins but with 1 order of magnitude bigger lattice spacings. Studies on such assemblies could lead to new class of materials including the extremely captivating "meta-materials".[10]

It is thus very important that we understand the formation and thermal behavior of the superlattices in as much detail as possible. The investigations dedicated so far to the temperature effects on the ligand protected metal nanoparticles and their superlattices can be categorized into two groups. The first ones are those focused on the order−disorder transitions of the self-assembled layers of the ligand shells capping individual nanoparticles vis-à-vis their bulk surfaces. For example, in many

*Correspondng author. E-mail: pl.bhagavatula@ncl.res.in. Ph: +91-20-25902013. Fax: +91-20-25902636.

(1) (a) Hutchings, G. J.; Brust, M.; Schmidbaur, H. *Chem. Soc. Rev.* **2008**, *37*, 1759. (b) Daniel, M. C.; Astruc, D. *Chem. Rev.* **2004**, *104*, 293. (c) Rosi, N. L.; Mirkin, C. A. *Chem. Rev.* **2005**, *105*, 1547. (d) Jain, P. K.; Huang, X.; El-Sayed, I. H.; El-Sayed, M. A. *Acc. Chem. Res.* **2008**, *41*, 1578. (e) Hu, M.; Chen, J.; Li, Z. Y.; Au, L.; Hartland, G. V.; Li, X.; Marquez, M.; Xia, Y. *Chem. Soc. Rev.* **2006**, *35*, 1084. (f) Murphy, C. J.; Gole, A. M.; Stone, J. W.; Sisco, P. N.; Alkilany, A. M.; Goldsmith, E. C.; Baxter, S. C. *Acc. Chem. Res.* **2008**, *41*, 1721. (g) Sidhaye, D. S.; Kashyap, S.; Sastry, M.; Hotha, S.; Prasad, B. L. V. *Langmuir* **2005**, *21*, 7979.
(2) Giersig, M.; Mulvaney, P. *Langmuir* **1993**, *9*, 3408.
(3) Brust, M.; Walker, M.; Bethell, D.; Schiffrin, D. J.; Whyman, R. *J. Chem. Soc., Chem. Commun.* **1994**, 801.
(4) (a) Zhang, S.; Leem, G.; Srisombat, L. O.; Lee, T. R. *J. Am. Chem. Soc.* **2008**, *130*, 113. (b) Schroedter, A.; Weller, H. *Angew. Chem., Int. Ed.* **2002**, *41*, 3218. (c) Lin, X. M.; Sorensen, C. M.; Klabunde, K. J. *Chem. Mater.* **1999**, *11*, 198. (d) Leff, D. V.; Ohara, P. C.; Heath, J. R.; Gelbart, W. M. *J. Phys. Chem.* **1995**, *99*, 7036. (e) Hu, Y.; Uzun, O.; Dubois, C.; Stellacci, F. *J. Phys. Chem. C* **2008**, *112*, 6279. (f) Jackson, A. M.; Hu, Y.; Silva, P. J.; Stellacci, F. *J. Am. Chem. Soc.* **2006**, *128*, 11135.
(5) (a) Badia, A.; Cuccia, L.; Demers, L.; Morin, F.; Lennox, R. B. *J. Am. Chem. Soc.* **1997**, *119*, 2682. (b) Badia, A.; Singh, S.; Demers, L.; Cuccia, L.; Brown, G. R.; Lennox, R. B. *Chem.—Eur. J.* **1996**, *2*, 359. (c) Bensebaa, F.; Ellis, T. H.; Badia, A.; Lennox, R. B. *Langmuir* **1998**, *14*, 2361.
(6) (a) Kiely, C. J.; Fink, J.; Brust, M.; Bethell, D.; Schiffrin, D. J. *Nature* **1998**, *396*, 444. (b) Prasad, B. L. V.; Sorensen, C. M.; Klabunde, K. J. *Chem. Soc. Rev.* **2008**, *37*, 1871. (c) Talapin, D. I. *ACS Nano* **2008**, *2*, 1097.
(7) (a) Pileni, M. P. *Acc. Chem. Res.* **2007**, *40*, 685. (b) Pileni, M. P. *Appl. Surf. Sci.* **2001**, *171*, 1. (c) Collier, C. P.; Vossmeyer, T.; Heath, J. R. *Annu. Rev. Phys. Chem.* **1998**, *49*, 371. (d) Murray, C. B.; Sun, S.; Gaschler, W.; Doyle, H.; Betley, T. A.; Kagan, C. R. *IBM J. Res. Dev.* **2001**, *45*, 47. (e) Wang, Z. L.; Harfenist, S. A.; Vezmar, I.; Whetten, R. L.; Bentley, J.; Evans, N. D.; Alexander, K. B. *Adv. Mater.* **1998**, *10*, 808. (f) Martin, J. E.; Wilcoxon, J. P.; Odinek, J.; Provencio, P. *J. Phys. Chem. B* **2000**, *104*, 9475. (g) Stoeva, S. I.; Prasad, B. L. V.; Uma, S.; Stoimenov, P. K.; Zaikovski, V.; Sorensen, C. M.; Klabunde, K. J. *J. Phys. Chem. B* **2003**, *107*, 7441.
(8) (a) Abecassis, B.; Testard, F.; Spalla, O. *Phys. Rev. Lett.* **2008**, *100*, 115504. (b) Andres, R. P.; Bielefeld, J. D.; Henderson, J. I.; Janes, D. B.; Kolagunta, V. R.; Kubiak, C. P.; Mahoney, W. J.; Osifchin, R. G. *Science* **1996**, *273*, 1690. (c) Santhanam, V.; Liu, J.; Agarwal, R.; Andres, R. P. *Langmuir* **2003**, *19*, 7881.
(9) (a) Shevchenko, E. V.; Talapin, D. V.; Kotov, N. A.; O'Brien, S.; Murray, C. B. *Nature* **2006**, *439*, 55. (b) Lu, C.; Chen, Z.; O'Brien, S. *Chem. Mater.* **2008**, *20*, 3594.
(10) (a) Smith, D. R.; Pendry, J. B.; Wiltshire, M. C. K. *Science* **2004**, *305*, 788. (b) Ponsinet, V.; Aradian, A.; Barois, P.; Ravaine, S. In *Metamaterials Handbook*, Capolino, F., Ed.; CRC Press: Boca Raton, FL, 2009.

 Published on Web 01/25/2010

elegant papers, the Lennox group has shown that the ligands form self-assembled monolayers on the nanoparticle surfaces similar to their bulk surfaces.[5] Special care has been taken in these studies to separate the nanoparticles from the excess thiol. Further, Landman and coworkers have studied such systems in a detailed manner and have shown that upon heating, these ligand shells undergo an order−disorder "melting" transition with the melting starting at the ligand tail, slowly propagating to the head attached to the nanoparticle surface.[11] Temperature dependence of dynamics of alkyl-chains in thiol protected metal cluster systems has been probed by the quasi-elastic neutron scattering and powder diffraction techniques.[12] The other class of studies consider melting of the nanoparticle superlattices.[13] These studies show that just like molecular and atomic crystals, superlattices of nanoparticles undergo melting point transitions. The popular choices for such studies have been gold and silver nanoparticles stabilized by thiols. However, in many instances, such studies also indicate the presence of excess thiol (sometimes even as high as 40 wt %, as compared to the expected 6−7 wt % calculated on the basis of single monolayer protection)[14] in the samples.

It has already been shown that superlattices of better quality could be grown from the monodisperse thiol-protected gold nanoparticles obtained by the highly effective "digestive ripening" process.[15] It has been seen that varying the alkanethiol chain length differentiates their propensity to form 3D superlattices. It was then concluded that as the chain length of the alkanethiol capping the nanoparticle increases, the attractive forces between the metal core decrease and hence nanoparticle with shorter chain length prefer to form 3D superlattices. We wish to mention here that based on the UV−vis and TEM studies, such structures have been shown to form in the solution itself.[15b] The presence of longer-chain-length thiol (hexadecane thiol for example) on the particle amounts to a decrease in the attractive forces and hence the particles remain isolated in solution with very little interaction. When films from such solutions are cast on a surface, two-dimensional hexagonal arrangement of the particles occurs due to the solvent evaporation. It has been unambiguously shown that the presence of excess thiol during the formation of superlattice structures helps in slowing down the formation process and hence better superlattice structures could be obtained.[9b,15,16] However, the way in which the presence of this excess thiol affects the melting characteristics has not been probed until date.

Here, we present a first comprehensive study on the thermal behavior of superlattices formed with gold nanoparticles capped by thiols of varying chain length. We also clearly establish that 3D superlattices formed from particles coated with shorter chain length thiols melt at higher temperatures as compared to superlattices formed by the particles capped with longer chain length thiols. Most importantly, whatever may be the thiol chain length, the formation of a 3D superlattice seems to occur only in presence of excess thiol.

Experimental Details

Chemicals. Dimethyldodecylammoniumbromide (DDAB), gold chloride ($AuCl_3$), 1-octanethiol ($C_8H_{17}SH$), 1-dodecanethiol ($C_{12}H_{25}SH$) and 1-hexadecanethiol ($C_{16}H_{33}SH$) were purchased from Sigma Aldrich while toluene, sodium borohydride ($NaBH_4$), ethanol (C_2H_5OH) and acetone (CH_3COCH_3) were purchased from Merck and used as received.

Preparation of Alkanethiol-Coated Gold Nanoparticles. The alkanethiol coated Au NPs were prepared following a procedure reported previously.[15b] To begin with, 0.02 M reverse micelle solution of dodecyldimethylammonium bromide (DDAB) was prepared by dissolving 0.2761 g dodecyldimethylammonium bromide (DDAB) in 30 mL of toluene. Then, 102 mg of $AuCl_3$ was added to this colorless solution. The solution turned dark orange after sonication. Then, aqueous solution $NaBH_4$ (108 μL, 9.4 M) was added with continuous stirring, which led to the formation of red colored solution. After stirring for 15 min. (ensuring completion of the reaction), this solution was divided into three parts of 10 mL each. Octanethiol was added to the first part, dodecanethiol to the second, and hexadecanethiol to the third such that in all the parts, the Au/thiol molar ratio was maintained to be 1:30. The reaction side products and excess reactants were removed by ethanol addition and the resultant precipitates were separated, dried and then redispersed in toluene to form a homogeneous solution. To these three solutions were once again added three alkanethiols, keeping the Au/thiol molar ratio at 1:30. Final solutions were then refluxed for 90 min under an argon atmosphere.

The three refluxed solutions were then cooled. In the case of octanethiol- and dodecanethiol-capped systems, precipitates started forming after leaving the sample vials undisturbed overnight. Such precipitates were carefully separated, thoroughly rinsed with cold ethanol several times, and subjected to further characterization. In the hexadecanethiol-capped case, no precipitation occurred even after waiting for long periods. Therefore, excess ethanol was added to the Au nanoparticle dispersions in toluene to cause precipitation. These precipitates were then washed as mentioned above and further studies were carried out. These precipitates would be designated as AuC_8SH, $AuC_{12}SH$ and $AuC_{16}SH$ for the octane, dodecane, and hexadecane−thiol cases, respectively. Additionally, part of the $AuC_{12}SH$ and $AuC_{16}SH$ samples were washed extensively with ethanol and acetone interspersed with sonication. These samples

(11) (a) Landman, U.; Luedtke, W. D. *Faraday Discu.* **2004**, *125*, 1. (b) Luedtke, W. D.; Landman, U. *J. Phys. Chem.* **1996**, *100*, 13323.
(12) (a) Mukhopadhyay, R.; Mitra, S.; Pradeep, T.; Tsukushi, I.; Ikeda, S. *J. Chem. Phys.* **2003**, *118*, 4614. (b) Mitra, S.; Nair, B.; Pradeep, T.; Goyal, P. S.; Mukhopadhyay, R. *J. Phys. Chem. B* **2002**, *106*, 3960. (c) Mukhopadhyay, R.; Mitra, S.; Johnson, M.; Kumar, V. R. R.; Pradeep, T. *Phys. Rev. B* **2007**, *75*, 75414. (d) Chaki, N. K.; Vijayamohanan, K. P. *J. Phys. Chem. B* **2005**, *109*, 2552.
(13) (a) Sandhyarani, N.; Resmi, M. R.; Unnikrishnan, R.; Vidyasagar, K.; Ma, S. G.; Antony, M. P.; Selvam, G. P.; Visalakshi, V.; Chandrakumar, N.; Pandian, K.; Tao, Y. T.; Pradeep, T. *Chem. Mater.* **2000**, *12*, 104. (b) Sandhyarani, N.; Antony, M. P.; Selvam, G. P.; Pradeep, T. *J. Chem. Phys.* **2000**, *113*, 9794. (c) Sandhyarani, N.; Pradeep, T.; Chakrabarti, J.; Yousuf, M.; Sahu, H. K. *Phys. Rev. B* **2000**, *62*, R739.
(14) Hostetler, J. M.; Templeton, A. C.; Murray, R. W. *Langmuir* **1999**, *15*, 3782.
(15) (a) Lin, X. M.; Sorensen, C. M.; Klabunde, K. J. *J. Nanoparti. Res.* **2000**, *2*, 157. (b) Prasad, B. L. V.; Stoeva, S. I.; Sorensen, C. M.; Klabunde, K. J. *Langmuir* **2002**, *18*, 7515. (c) Narayanan, S.; Wang, J.; Lin, X. M. *Phys. Rev. Lett.* **2004**, *93*, 135503–1.
(16) Korgel, B. A.; Fitzmaurice, D. *Phys. Rev. Lett.* **1998**, *80*, 3531.

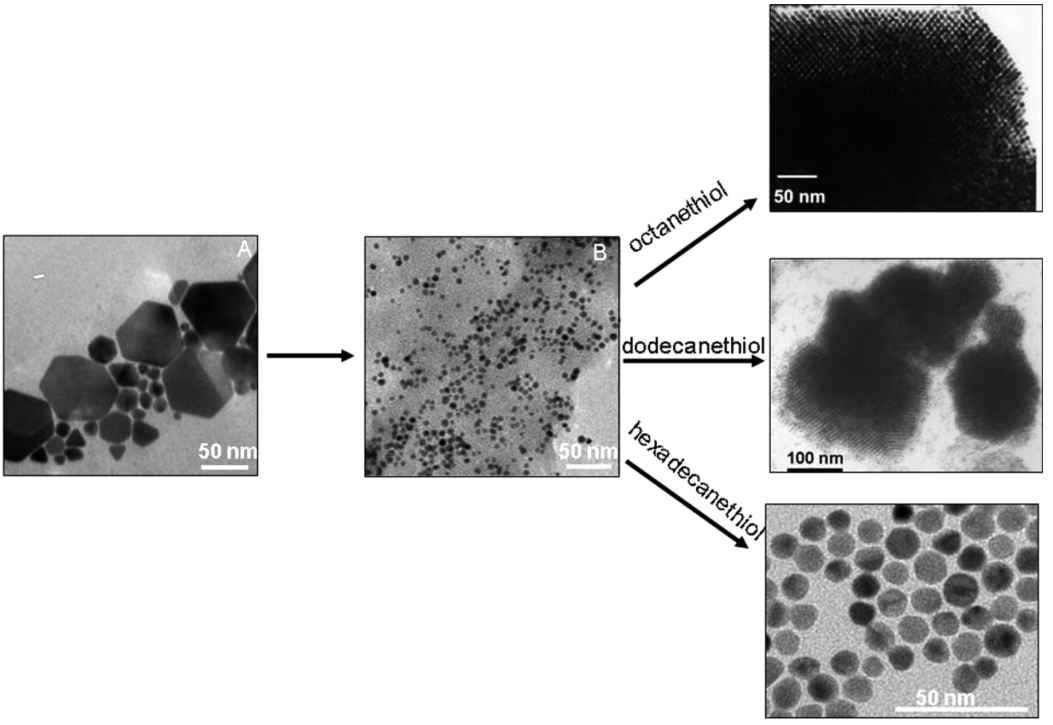

Figure 1. Scheme depicting the digestive ripening process and the TEM images of the ensuing superlattices with octanethiol and dodecanethiol capped nanoparticles. Note the absence of superlattice structures in the hexadecanethiol-capped nanoparticle case.

would be designated as $AuC_{12}SH$-w and $AuC_{16}SH$-w, respectively. All the samples were kept in vacuum desiccators and were used for further studies.

Instrumental Details. *TEM and Electron Diffraction Measurements*. Samples for transmission electron microscopy (TEM) were prepared by drop coating on carbon-coated copper grids. TEM analysis was performed on (1) JEOL model 1200EX instrument operated at an accelerating voltage at 120 kV and (2) TECHNAI G2 F30 S-TWIN instrument operated at an acceleration voltage of 300 kV with a lattice resolution of 0.14 nm and a point image resolution of 0.20 nm.

Differential Scanning Caloriemetry. Melting characteristics were studied using Mettler -Toledo DSC 821^e (Mettler−Toledo, Switzerland) equipped with intracooler. Indium/Zinc standards were used to calibrate DSC temperature and enthalpy scale. The samples were weighed and hermetically sealed in aluminum pans and heated and cooled at a constant rate of 5 °C/min, over a temperature of (i) 25−200 °C, (ii) 25−300 °C. An inert atmosphere was maintained by purging nitrogen gas (flow rate, 50 mL min^{-1}).

Thermogravimetric Analysis. The TGA experiments were carried out on a Mettler Toledo TGA Instrument (TGA/SDTA 851^e) controlled by STAR^e software (Mettler Toledo GmbH, Switzerland). Dry sample powders were placed in ceramic crucible and analyzed over the temperature range of 32−800 °C at the rate of 10 °C min^{-1} under the dry flow of N_2 at a rate of 30 mL min^{-1}.

XPS Analysis. XPS measurements were carried out on a VG MicroTech ESCA 3000 instrument at a pressure better than 10^{-9} Torr. The spectra were recorded with unmonochromatized Mg*K*α radiation (photon energy = 1253.6 eV) at a pass energy of 50 eV, electron takeoff angle (angle between electron emission direction and surface plane) of 60°, and a resolution of 0.1 eV.

Results

As mentioned earlier, the making of the monodisperse particles and the formation of superlattices has been accomplished by the "digestive ripening" procedure following the published reports.[15b] We could faithfully repeat the results as obtained in the earlier reports and the results are summarized in Scheme 1 (see Figure 1). From the results, it could be concluded that Au nanoparticles capped by short chain length thiols (octane and dodecane) show a better propensity to form 3D superlattices. On the other hand, in the case of hexadecane thiol capping, the particles remain isolated in solution. These form two-dimensional hexagonal close-packed arrangements when drop-casted on a surface as the particles come closer because of the solvent evaporation.

We wish to remind here that when solutions of Au nanoparticles capped by octane or dodecanethiol are kept undisturbed in the vials, waxy precipitates could be seen at the bottom of the sample vials. Such precipitates were isolated and washed carefully with cold ethanol. These were labeled AuC_8SH and $AuC_{12}SH$ respectively. Solutions of nanoparticles capped by hexadecanethiol do not reveal the presence of any precipitate. However, upon addition of excess ethanol, black precipitates of nanoparticles capped by hexadecanethiol could indeed be obtained. The precipitate so obtained was again washed with cold ethanol and was labeled $AuC_{16}SH$. To ascertain the composition, i.e., organic material vs gold content present in these systems, the above precipitates were subjected to thermogravimetric analysis (TGA). Figure 2A shows TGA curves for sample $AuC_{16}SH$, $AuC_{12}SH$, and AuC_8SH. The weight losses obtained are 62% ($AuC_{16}SH$), 25% ($AuC_{12}SH$), and 23% (AuC_8SH).

Such weight losses could be attributed to the presence of surfactant (DDAB) or the digestive ripening agents (thiols) used to prepare these ligand capped particles. To

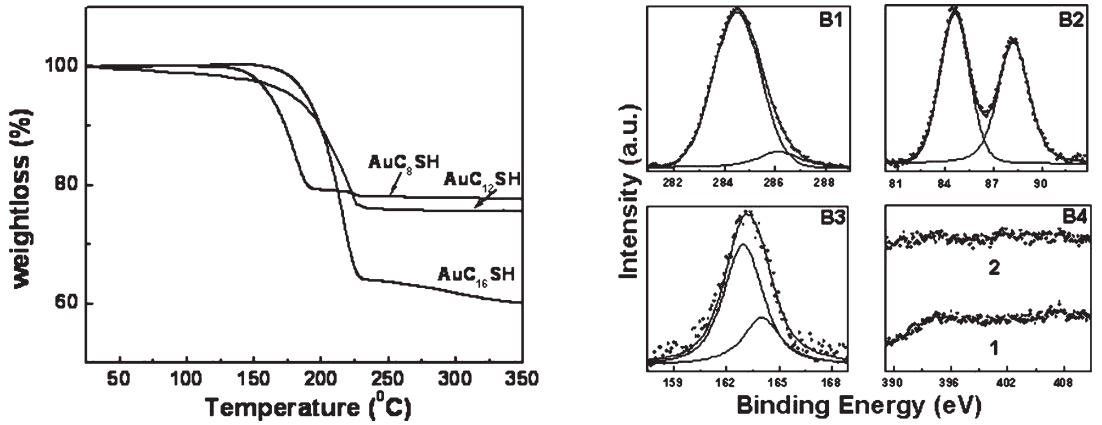

Figure 2. (A) Thermogravimetric analyses of the gold nanoparticle superlattice structures capped by alkanethiols of varying chain length. (B1) C-1s XPS spectrum corresponding to the sample $AuC_{16}SH$, (B2) Au-4f XPS spectrum corresponding to the sample $AuC_{16}SH$, (B3) S-2p XPS spectrum corresponding to the sample $AuC_{16}SH$, (B4) N-1s XPS spectra corresponding to the sample $AuC_{16}SH$ (curve 1) and to sample $AuC_{12}SH$ (curve 2).

see which one of them mainly contributed to the weight loss, samples $AuC_{16}SH$ and $AuC_{12}SH$ were subjected to XPS Analysis. The spectra were recorded from films of the samples prepared by drop coating on to Si (111) wafers. The C 1s, Au 4f, S 2p core level spectra recorded from sample Au−$C_{16}SH$ are shown in Figure 2 B1, B2, and B3 respectively. The spectra from C 1s, Au 4f, and S 2p core levels in sample $AuC_{12}SH$ were almost similar to those of sample $AuC_{16}SH$ and hence are not presented here for brevity. All the spectra have been background corrected using the Shirley algorithm prior to curve resolution.[17] The core levels were aligned with respect to the adventitious C 1s BE of 284.6 eV. The C1s core level spectrum could be deconvolutated into two components corresponding to the adventitious carbon and the carbon attached to the sulfur atom in the alkanethiol. The Au 4f core level could be stripped into a spin−orbit pair ($Au4f_{7/2}$ and Au $4f_{5/2}$) displaying a splitting of 3.7 eV. The S 2p core level signal could be resolved into two peaks corresponding to $S2p_{3/2}$ and $S2p_{1/2}$. The spectra could be fitted by ~2:1 peak area ratio and ~1.2 eV splitting. Interestingly, the photoelectron emission from the N1s core levels of both the samples resulted in a noisy signal (Figure 2 B4) and any detailed analysis as done for other elements could not be done, indicating that the presence of nitrogen and hence the surfactant present in the material is quite negligible.

The melting characteristics of the samples were studied by Differential Scanning caloriemetry (DSC) and visual inspection. The temperature variation was done in two ways. The analysis was started at room temperature in both the methods. In the first instance, the samples were heated to 200 °C and then cooled back to room temperature. This cycle was repeated once more but this time the temperature was increased up to 300 °C and then cooled back to room temperature. For the sake of clarity, we present first the results of the room temperature−200 °C−room temperature cycle (Figure 3). It can be clearly seen that an endothermic peak could be seen at ~145 °C (for AuC_8SH), ~130 °C (for $AuC_{12}SH$), and ~55 °C (for $AuC_{16}SH$). We wish to inform that during several repetitions of these experiments, we noticed the trends to be the same every time, although the endothermic peaks do not occur exactly at the same points every time. From the visual inspection details (Table 1), such endothermic peak could be related to the melting of superlattices. So it can be noticed that as the chain length of thiol present on the nanoparticle surface increases, the endothermic peak occurs at a lower temperature.

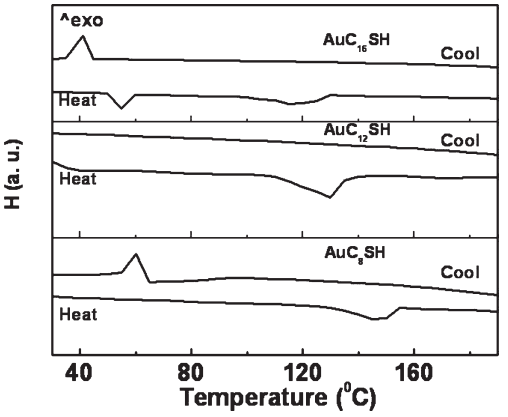

Figure 3. DSC analyses of the gold nanoparticle superlattice structures capped by alkanethiols of varying chain length.

Table 1. Visual Inspection Details of Melting of Gold Nanoparticle Superlattices with Different Alkane Chain Lengths Investigated in This Study

	temperature (°C)		
sample	solid to liquidlike	liquid to goldenlike solid	boiling point of the capping agent
AuC_8SH	145−150	~215	197−200
$AuC_{12}SH$	125−130	~215	266−283
$AuC_{16}SH$	50−60	~215	~350

The most interesting results are seen in $AuC_{12}SH$-w (excess washed) sample. In this case, the precipitates described earlier as $AuC_{12}SH$ were washed thoroughly with combinations of ethanol and acetone interspersed with sonication. Such excess washing would have removed any free thiol and indeed the TGA analysis of the $AuC_{12}SH$-w (Figure 4A) sample reveals only 13%

(17) Shirley, D. A. *Phys. Rev. B.* **1972**, *5*, 4709.

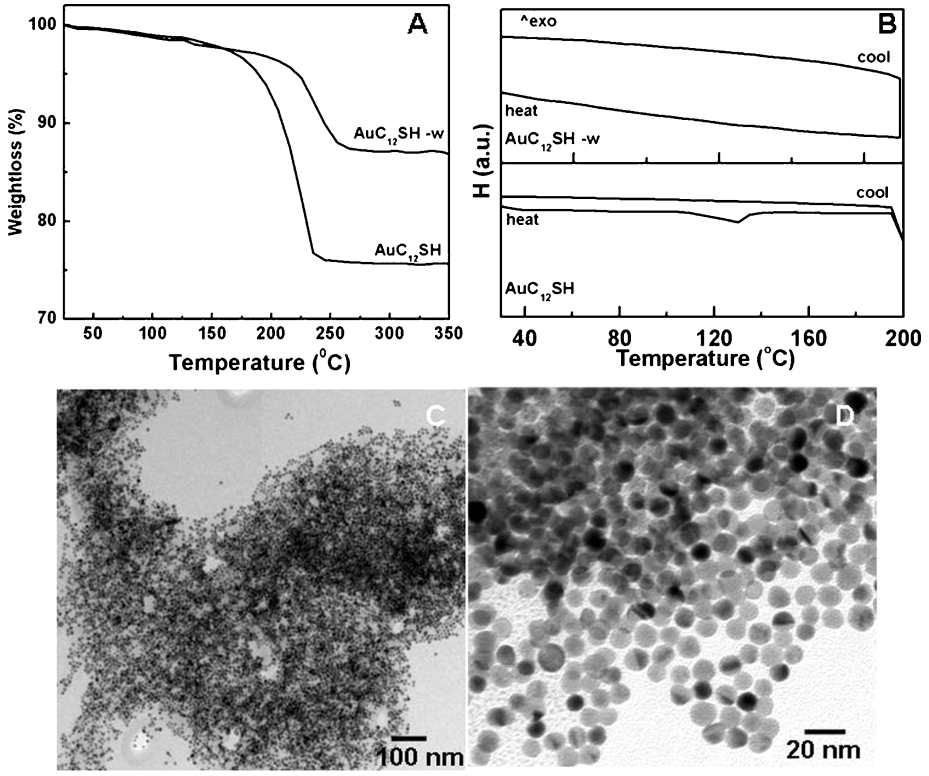

Figure 4. (A) TGA curves for sample $AuC_{12}SH$ and thoroughly washed sample $AuC_{12}SH$-w. (B) (lower panel) DSC traces of the dodecanethiol-coated gold nanoparticle superlattice structures ($AuC_{12}SH$); (upper panel) DSC traces of the dodecanethiol-coated gold nanoparticle superlattice structures after thorough washing ($AuC_{12}SH$-w). The traces are recorded in the room temperature−200 °C−room temperature cycle. (C, D) TEM images of the sample $AuC_{12}SH$-w. Notice the absence of any 3D or 3D-ordered structures in these images.

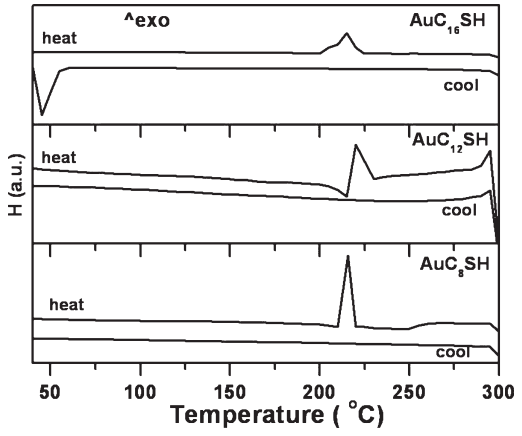

Figure 5. DSC analysis curves of the different alkanethiol coated gold nanoparticles in the room temperature−300 °C−room temperature cycle.

weight loss. What is interesting to note is the complete absence of any endothermic peak in the DSC graphs obtained from this Au−C_{12}SH-w (Figure 4B, upper panel) sample. TEM images of this sample (when the washed precipitate was resuspended in toluene and drop casted on a TEM grid) reveal no superlattices (Figure 4C,D).

To gain further knowledge on the stability of such superlattice structures with respect to temperature, we repeated the DSC experiments in the following cycle: room temperature−300 °C−room temperature. Here, in all the samples (regardless of the thiol chain length), an exothermic peak around 215 °C could be seen (Figure 5).

Discussion

Thus, results obtained can be explained as follows. Monodisperse nanoparticles capped by short alkane chain length thiols form 3D superlattices, while those with longer chain length do not form any superlattice structures in solution. This has been attributed to the greater attractive forces between the metal cores, which are of the order of 5 k_BT and 2 k_BT, respectively, for the octane thiol and dodecanethiol cases respectively. On the other hand, because of the weak attractive forces between the metal cores (magnitude of attractive forces 0.6 k_BT) in the hexadecanethiol case, the particles remain isolated in solution.[15b] The DSC analysis presented here reveals that when superlattices obtained from nanoparticles capped by octane, dodecane, and hexadecane−thiol are heated; an endothermic peak is observed, which occurs at lower temperatures as the chain length of thiol increases. Taking a clue from earlier reports[13] and the visual observations (Table 1), it can be safely concluded that such endothermic peaks are evidence of superlattice melting. Therefore, the longer the alkane chain length, the superlattice melting occurs at lower temperature.

It is noteworthy that in the TGA analysis of AuC_8SH, $AuC_{12}SH$, and $AuC_{16}SH$ samples, the weight loss is higher than expected (a 6−7 wt % weight loss is expected if the thiol were forming a simple monolayer on the surface of nanoparticle).[14] From the XPS analysis, this excess weight loss is attributed to the presence of excess thiol molecules and not the surfactant. This is not surprising

because in the digestive ripening procedure, the polydispersed particles prepared in the presence of the surfactant are first broken into small spherical particles by addition of thiol, which could have replaced any surfactant capping these polyhedral, polydisperse systems contain. These are then isolated by precipitation and refluxed with excess thiol. Thiols are known to bind very strongly to gold surface and place exchange any weakly bound molecules.[18] Thus in the second step of digestive ripening where the particles are refluxed with excess thiol, the DDAB remaining, if any, on the spherical particles would get removed. This is supported by the XPS results where the signal from N 1s core level is very weak as compared to signals from other elements. In fact, our results are quite similar to those reported by Schiffrin and co-workers.[19] They have also seen very weak N 1s signals after purifying the thiol-protected particles (prepared by the celebrated Brust-Schiffrin two-phase synthesis method) by Soxhlet extraction.

The above XPS analysis and the TEM results thus clearly prove that excess thiol plays a major role in the formation of superlattice structures. So what would happen if we remove this excess thiol? We therefore subjected the sample Au−C_{12}SH to repeated washings with acetone and ethanol accompanied by sonication. Such thoroughly washed samples revealed a weight loss of 13%, which is closer to that expected for a single monolayer of thiol present on particles we prepared. Most interestingly, the endothermic peak (DSC) and ordered assembly formation (TEM analysis) seen in the sample Au−C_{12}SH are absent in the Au−C_{12}SH-w sample, clearly indicating the nonexistence of superlattice formation.

We infer that the exothermic peak at 215 °C (Figure 5) when the samples are heated to above 200 °C corresponds to the thiol desorption from the particle surface. As breaking of the Au−S bond is not expected to be influenced much by the chain length of thiol, we see the peak at same position irrespective of the thiol chain length. Though it is surprising to see an exothermic peak associated with thiol desorption from nanoparticle surface, we assume that such desorption could be accompanied by disulfide formations leading to over all exothermicity.

We also wish to mention here that in the cooling cycle of the DSC experiments (200 °C−room temperature), the peaks that can be associated with the reformtion of superlattices occur at much lower temperatures than the melting peak. The melting of the superlattices reported here is much different than the melting in normal atomic/molecular systems. As each of the particle participating in the superlattice formation is much bigger than the atomic/molecular systems the superlattices could be forming at much longer time scales than the DSC cooling rates and freezing transitions are anyway known to be stochastic. However, such samples were redispersible in solvents such as toluene suggesting that the thiol capping is still intact on the particle surfaces. On the other hand, samples obtained after heating them to 300 °C were sticking to the DSC pans and could not be resuspended in toluene supporting the thiol desorption hypothesis.

There are a few questions still unanswered. From the reports[6] and from our own study presented here, it is firmly established that superlattice formation occurs in the presence of excess thiol. It is also reported that the thiol molecules adsorbed on the surface of nanoparticles are in a dynamic equilibrium with those present in solution.[14,18] Such thiol is known to slowdown the evaporation process either on the TEM grid or even in solution, thus resulting in better superlattices. But, a rather different picture emerges from the TEM analysis. In almost all the TEM images of Au nanoparticle superlattices published so far the average distance between two neighboring particles is revealed to be less than twice the length of the capping thiol molecule indicating an appreciable degree of interdigitation. Now, if the superlattice formation almost exclusively happens in presence of excess thiol where is this excess thiol going after superlattice formation? What are the dynamics between this excess thiol and the thiol molecules capping the nanoparticle surface during and immediately after the superlattice formation? We do not have any answers to these questions right now. However, we believe that the free thiol that aids in the superlattice formation gets "excluded" as the particles come together. But this thiol probably gets trapped in the interstitial sites of the fcc superlattice (close packing of the spheres in fcc lattice occupies only 74% volume) and in between the precipitates which are nothing but the loosely packed structures of the superlattices. Such thiol appears to play an important role not only in the formation of superlattices but in their melting as well.

Conclusion

In conclusion, gold nanoparticles coated with alkanethiols of different chain-length (octane, dodecane and hexadecane) have been synthesized. Melting properties of superlattices obtained from these samples are studied. The results of the washed and unwashed samples reveal that free "excess thiol" is important for the formation of good superlattices and indeed plays an important role in their melting characteristics also. From this, we feel that if the proportion of the excess alkanethiol can be tuned, the formation of superlattices could be controlled, paving the way for better realization of their applications.

Acknowledgment. D.S. acknowledges CSIR for fellowship. BLVP thanks the Department of Science and Technology (DST) for funding through DST-UNANST (Unit on Nanoscience and Technology) at NCL. BLVP earnestly thanks Prof. Kenneth Klabunde and Prof. Chris Sorensen for their constant encouragement and support.

(18) (a) Hostetler, M. J.; Wingate, J. E.; Zhong, C. −J.; Harris, J. E.; Vachet, R. W.; Clark, M. R.; Londono, J. D.; Green, S. J.; Stokes, J. J.; Wignall, G. D.; Glish, G. L.; Porter, M. D.; Evans, N. D.; Murray, R. W. *Langmuir* **1998**, *14*, 17. (b) Hasan, M.; Bethell, D.; Brust, M. *J. Am. Chem. Soc*. **2002**, *124*, 1132.
(19) Waters, C. A.; Mills, A. J.; Johnson, K. A.; Schiffrin, D. J. *Chem. Commun*. **2003**, 540.